



# Evaluation of VIIRS, GOCI, and MODIS Collection 6 AOD retrievals against ground sunphotometer observations over East Asia

Q. Xiao<sup>1</sup>, H. Zhang<sup>2</sup>, M. Choi<sup>3</sup>, S. Li<sup>1,4</sup>, S. Kondragunta<sup>5</sup>, J. Kim<sup>3</sup>, B. Holben<sup>6</sup>, R. C. Levy<sup>6</sup>, and Y. Liu<sup>1</sup>

<sup>1</sup>Department of Environmental Health, Rollins School of Public Health, Emory University, Atlanta, GA, USA

<sup>2</sup>I.M. Systems Group Inc., College Park, MD, USA

<sup>3</sup>Department of Atmospheric Sciences, Yonsei University, Seoul, South Korea

<sup>4</sup>State Key Laboratory of Remote Sensing Science, Beijing, China

<sup>5</sup>National Oceanic and Atmospheric Administration, Greenbelt, MD, USA

<sup>6</sup>NASA Goddard Space Flight Center, Greenbelt, MD, USA

Correspondence to: Y. Liu (yang.liu@emory.edu)

Received: 23 June 2015 – Published in Atmos. Chem. Phys. Discuss.: 3 August 2015

Revised: 13 January 2016 – Accepted: 14 January 2016 – Published: 3 February 2016

**Abstract.** Persistent high aerosol loadings together with extremely high population densities have raised serious air quality and public health concerns in many urban centers in East Asia. However, ground-based air quality monitoring is relatively limited in this area. Recently, satellite-retrieved Aerosol Optical Depth (AOD) at high resolution has become a powerful tool to characterize aerosol patterns in space and time. Using ground AOD observations from the Aerosol Robotic Network (AERONET) and the Distributed Regional Aerosol Gridded Observation Networks (DRAGON)-Asia Campaign, as well as from handheld sunphotometers, we evaluated emerging aerosol products from the Visible Infrared Imaging Radiometer Suite (VIIRS) aboard the Suomi National Polar-orbiting Partnership (S-NPP), the Geostationary Ocean Color Imager (GOCI) aboard the Communication, Ocean, and Meteorology Satellite (COMS), and Terra and Aqua Moderate Resolution Imaging Spectroradiometer (MODIS) (Collection 6) in East Asia in 2012 and 2013. In the case study in Beijing, when compared with AOD observations from handheld sunphotometers, 51 % of VIIRS Environmental Data Record (EDR) AOD, 37 % of GOCI AOD, 33 % of VIIRS Intermediate Product (IP) AOD, 26 % of Terra MODIS C6 3 km AOD, and 16 % of Aqua MODIS C6 3 km AOD fell within the reference expected error (EE) envelope ( $\pm 0.05 \pm 0.15$  AOD). Comparing against AERONET AOD over the Japan–South Korea region, 64 % of EDR, 37 % of IP, 61 % of GOCI, 39 % of Terra MODIS, and 56 % of Aqua

MODIS C6 3 km AOD fell within the EE. In general, satellite aerosol products performed better in tracking the day-to-day variability than tracking the spatial variability at high resolutions. The VIIRS EDR and GOCI products provided the most accurate AOD retrievals, while VIIRS IP and MODIS C6 3 km products had positive biases.

## 1 Introduction

Aerosols play a critical role in atmospheric processes as well as global climate change. Rapid economic growth and increasing fossil fuel usage have significantly affected aerosol formation and transportation in East Asia. From 1980–2003, the emissions of black carbon, organic carbon, SO<sub>2</sub>, and NO<sub>x</sub> increased by 28, 30, 119, and 176 %, respectively (Ohara et al., 2007). Aerosols are also noted for their adverse health impacts, such as increased cardiovascular and respiratory morbidity and mortality (Lim et al., 2013). The continuous air quality degradation together with high population density have raised serious public health concerns in East Asia.

Satellite remote-sensing data have been applied to characterize aerosol global distribution and temporal variation. Although the primary goal of satellite observations is to advance our understanding of the climate system, the comprehensive spatial coverage and growing time series of satellite

retrievals benefit various applications, including monitoring ground level air pollution, especially particulate matter (PM). The traditional ground-based air quality monitoring networks are expensive to operate and have limited spatial coverage. For example, most PM monitoring stations in China are located in urban centers and the monitoring network only covers about 360 out of the more than 3000 counties. Most developing countries, where PM levels are dangerously high, have little or no regular ground monitoring network. These limitations of ground measurements result in insufficient information to conduct studies about pollution sources, distribution, and consequent health impacts. Satellites provide continuous, high-coverage observations of aerosol loadings and various approaches have been developed to estimate ground-level PM concentrations from satellite retrievals (Ma et al., 2014; Xu et al., 2015). Estimates of ground-level PM concentrations from satellite observations have been used in epidemiological studies and benefited policy making (Strickland et al., 2015; Evans et al., 2013).

The most widely used satellite aerosol sensor, the Moderate Resolution Imaging Spectroradiometer (MODIS), has 36 spectral bands, acquiring data in wavelength from 0.41 to 15  $\mu\text{m}$  and providing information about atmospheric aerosol properties (Anderson et al., 2003). Two identical MODIS instruments are aboard the National Aeronautics and Space Administration (NASA) Terra and Aqua satellites, which fly over the study area at around 10:30 and 13:30 LT, respectively. Several algorithms have been developed to retrieve aerosol optical depth (AOD) from MODIS data over land, such as the Dark-Target (Levy et al., 2013) algorithm and the Deep-Blue (Hsu et al., 2013) algorithm, providing AOD retrievals at 550 nm with global coverage. The widely used 10 km resolution MODIS aerosol products provides valuable information on aerosol distribution in space and time, and has been widely used to characterize aerosol dynamics and distribution, simulate climate change, and assess population PM exposure (Levy et al., 2010, 2013). However, the 10 km product cannot depict small-scale PM heterogeneity. Though a previous study (Anderson et al., 2003) indicated that the aerosol loading is homogeneous at horizontal scales within 200 km, that study is conducted over the ocean, which provides a homogeneous surface, leading to reduced aerosol spatial variability. The variability of aerosol loading at local scales in urban areas with complex land surface and meteorological conditions is expected to be greater (Li et al., 2005). Accurately characterizing local-scale aerosol heterogeneity is critical for assessing population PM exposure, detecting small smoke plums, and analyzing aerosol-cloud process. To resolve small-scale aerosol features, satellite aerosol products with higher resolutions and accuracy are urgently needed.

In response to the requirement of aerosol retrievals with higher spatial resolution, several emerging satellite aerosol products have become available recently. The Visible Infrared Imaging Radiometer Suite (VIIRS) is a multi-

disciplinary scanning radiometer with 22 spectral bands covering from 0.412 to 12.05  $\mu\text{m}$  and is designed as a new generation of operational satellite sensors that are able to provide aerosol products with a similar quality to MODIS (Jackson et al., 2013). VIIRS is on board the NASA-NOAA Suomi National Polar-orbiting Partnership (S-NPP) that launched in October 2011, and passes over the study area daily at approximately 13:30 LT. The VIIRS aerosol product reached provisional maturity level in January 2013, which means the “product quality may not be optimal” but it is “ready for operational evaluation” (Liu et al., 2014). The characteristics of the instrument and the aerosol retrieval algorithms are documented in detail elsewhere (Liu et al., 2014) and briefly described here. VIIRS provides two AOD products: the Intermediate Product (IP) and the Environmental Data Record (EDR). The VIIRS aerosol retrieval is performed at pixel-level ( $\sim 0.75$  km) spatial resolution globally as the IP that employs information from Navy Aerosol Analysis and Prediction System (NAAPS) and Global Aerosol Climatology Project (GACP) to fill in missing observations (Vermote et al., 2014). The IP is then aggregated to 6 km spatial resolution as the EDR, a level 2 aerosol product, through quality checking and excluding information from the NAAPS and GACP models. Both VIIRS IP and EDR are assigned quality flags of “high”, “degraded”, or “low” and valid AOD values range between 0.0 and 2.0. Detailed description of the quality assurance of VIIRS aerosol products is documented by Liu et al. (2014). Previous global evaluation against AERONET AOD over all land use types indicates that 71 % of EDR retrievals fell within the expected error (EE) envelope established by MODIS level 2 aerosol products over land ( $\pm 0.05 \pm 0.15$  AOD), with a bias of  $-0.01$  (Liu et al., 2014).

The Geostationary Ocean Color Imager (GOCI) is a geostationary Earth orbit sensor, providing hourly multi-spectral aerosol data eight times per day from 09:00 to 16:00 Korean LT. It covers a  $2500 \times 2500$  km<sup>2</sup> sampling area, centered at [130° E, 36° N] in East Asia, at 500 m resolution with eight spectral channels at 412, 443, 490, 555, 660, 680, 745, and 865 nm, respectively (Park et al., 2014). GOCI is aboard South Korea’s Communication, Ocean, and Meteorology Satellite (COMS) that launched in June 2010. The retrieval algorithm of its aerosol product, Yonsei aerosol retrieval algorithm, was originally based on the NASA MODIS algorithm and provides level 2 AOD retrievals at 6 km spatial resolutions (Levy et al., 2007, 2010; Lee et al., 2010). The characteristics of the Yonsei retrieval algorithms and the aerosol product are documented in detail by Choi et al. (2015). The GOCI aerosol product allows AOD values ranging between  $-0.1$  and 5.0. A previous study reported that during a 2-month period (1 April to 31 May 2011), the GOCI AOD retrievals agreed well with AERONET AOD ( $R^2 = 0.84$ ) over East Asia (Park et al., 2014). A recently published evaluation study reported that from March to May 2012, the GOCI AOD had a linear relationship with

AERONET AOD with a slope of 1.09 and an intercept of  $-0.04$  (Choi et al., 2015).

To meet the need for finer resolution aerosol products, a 3 km aerosol product was introduced as part of the MODIS Collection 6 delivery. The 3 km aerosol product includes a quality flag ranging between 0 and 3 to indicate the quality of each retrieval and the valid AOD values range between  $-0.1$  and 5.0. The retrieval algorithm of the 3 km product is documented in detail by Remer et al. (2013) and a global evaluation based on 6 months of Aqua data against ground sunphotometer AOD indicates that 63 % of the retrievals fell into the EE with a bias of 0.03 over land (Remer et al., 2013). Munchak et al. (2013) reported that in the Baltimore–Washington, DC area, an urban/suburban region, 68 % of the 3 km retrievals from 20 June 2011 to 31 July 2011 fell into the EE with a bias of 0.013.

The release of these fine-resolution satellite aerosol products has raised the question of whether these AOD retrievals can reflect the spatial pattern of aerosol loadings at their assigned resolutions. AERONET, a globally distributed federation of ground-based atmospheric aerosol observations, provides reliable “ground truth” of AOD that are widely used for the characterization of aerosol and validation of satellite retrievals (Morys et al., 2001; Holben et al., 1998). However, previous evaluation studies comparing these emerging satellite aerosol retrievals with AERONET data were mostly at the global scale. AOD retrievals and their errors are treated as spatially independent because the validation sites are far apart and the AOD retrieval resolutions are relatively low. Therefore, these studies evaluated how accurately a satellite product can track AOD values in time. With the help of spatially dense ground measurements, a regional-scale evaluation can evaluate satellite aerosol products’ abilities to accurately reflect the fine-scale aerosol characteristics in space. In response to the lack of spatially concentrated ground AOD observations, AERONET conducted several campaigns, which temporarily deployed additional sunphotometers in selected regions and provided valuable information on small-scale AOD distribution. One of these campaigns, the Distributed Regional Aerosol Gridded Observation Network (DRAGON)-Asia Campaign in Japan and South Korea, lasted from 15 February 2012 to 31 May 2012 and provided a rare opportunity to validate these emerging satellite aerosol products in East Asia (Seo et al., 2015; Sano et al., 2012). Another issue with previous evaluation studies is that few of them focused specifically on urban areas with higher pollution levels, greater disease burdens, and more complex aerosol patterns. Our work contributes to the validation effort of these emerging satellite products by employing ground AOD observations at finer resolution, extending the study period to 1 year, and conducting a mobile sampling experiment in the urban core of Beijing.

In this work, we quantitatively evaluate whether the latest VIIRS, GOCI and MODIS aerosol products can provide reliable AOD retrievals and accurately characterize the spatial

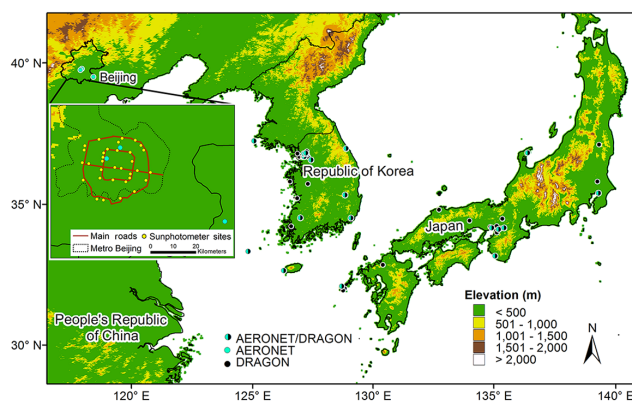


**Figure 1.** Study area showing all the ground AOD measurement sites.

pattern of AOD over the urban areas in East Asia. Ground AOD from AERONET, DRAGON-Asia, and handheld sunphotometers were collected over a period of 1 and a half years. The rest of the paper is organized such that Sect. 2 describes data sources and evaluation methods used in this study, Sect. 3 presents the performance of various satellite AOD products in representing intra city as well as regional variability of aerosol loadings. Finally, we summarize our findings and described future study directions in Sect. 4.

## 2 Data and methods

### 2.1 Study area

The extent of the study area is approximately  $2500 \times 1100 \text{ km}^2$ , centered at  $[128.5^\circ \text{ E}, 35.5^\circ \text{ N}]$  in East Asia, covering eastern China, South Korea, and Japan (Fig. 1). This domain is within the overlapping region of all satellite data sets and ground observations and covers large urban centers, suburban areas, and rural areas. We also conducted a mobile sampling study in Metro Beijing along three major roads (Fig. 1). The study period is from January 2012 to June 2013.

### 2.2 Remote-sensing data

The satellite aerosol products used in this study were from VIIRS, GOCI, Aqua MODIS and Terra MODIS sensors (Table 1). VIIRS data before May 2012 are not available because the sensor was in an early checkout phase and lacked a validated cloud mask (Liu et al., 2014). Thus, only EDR and IP pixels from May 2012 to June 2013 with high-quality (Quality Flag = “high”) were processed. Similarly, GOCI aerosol retrievals from January 2012 to June 2013 were filtered by its assigned quality and only high quality (Quality Flag = 3) retrievals were included. The Aqua and Terra MODIS C6 3 km data from January 2012 to June 2013 were obtained from the Goddard Space Flight Center (<http://>

//adsweb.nascom.nasa.gov/data). Only retrievals with high quality (Quality Flag = 3) were included in the analysis. The quality control criteria of these five satellite aerosol products are shown in Table 1.

### 2.3 Ground observations

The characteristics of ground AOD data sets are shown in Table 2. There were 18 permanent AERONET stations in the study area during the study period, supplemented by 24 temporary stations during the DRAGON-Asia Campaign. The DRAGON stations were distributed nearly uniformly with approximately 10 km apart from each other in two urban centers: Osaka in Japan (7 stations) and Seoul in South Korea (11 stations). Other DRAGON stations, which can be tens to hundreds of kilometers apart, were located across Japan and South Korea. The sunphotometer at each AERONET station measures AOD at eight spectral bands between 340 and 1020 nm. To compare with satellite retrievals, AOD at 550 nm was calculated using a quadratic log-log fit from AERONET AOD at wavelengths 440 and 675 nm. Near-real time level 2.0 AERONET/DRAGON data in the Japan–South Korea region and level 1.5 AERONET data in Beijing were downloaded from the Goddard Space Flight Center (<http://aeronet.gsfc.nasa.gov/>). The Level 2.0 (quality assured) AOD data have both pre- and post-deployment calibration, leading to an uncertainty of about 0.01–0.02 while the Level 1.5 AOD data are cloud-screened but not quality-assured (Otter et al., 2002). However, our preliminary results indicate that the level 1.5 daily average AOD values agreed well with the level 2.0 data, with a slope of 1.0 and zero intercept. Thus, we used the level 1.5 data in the case study in Beijing because level 2.0 data are not available for some AERONET stations.

To analyze the intra-city aerosol variability, we conducted ground measurements of AOD by a handheld sunphotometer (model 540 Microtops II, Solar Light Company, Inc.) at the Metro Beijing area in 2012 and 2013. Microtops II provide accurate AOD retrievals and is widely used for ground AOD observations (Morys et al., 2001; Tiwari and Singh, 2013; Otter et al., 2002). Previous calibration reported that the root-mean square differences in AOD from Microtops and corresponding AERONET stations were about  $\pm 0.02$  at 340 nm (Ichoku et al., 2002). In this study, ground observations were conducted on every cloud-free day at preselected sites that were roughly 6 km apart from each other along the 3rd and the 5th Ring Roads and the Chang'an Avenue of Beijing. This sampling took place between 09:30 and 14:00 LT, and 5–10 repeated measurements were made at each site. To control the quality of the ground data, we used the median value of the repeated observations as ground truth to eliminate the impact of extreme values and only included AOD with the ratio of standard deviation over median AOD less than 2.0. Our comparison of Microtops AOD retrievals with nearby

AERONET data yielded a slope of  $\sim 0.95$  and a correlation coefficient of  $\sim 0.8$  (Supplement, Text S1).

### 2.4 Data integration and analytical methods

Since satellite pixel coordinates are provided in a geographic coordinate system, to acquire the accurate Euclidean distance between satellite pixels and ground measurement locations, the coordinates of all the data were converted to the JGD\_2000\_UTM\_Zone\_52N coordination system. For a matchup process, a 6 km grid and a 3 km grid covering the whole study domain were constructed, corresponding to the spatial resolution of each satellite product. Satellite aerosol data from different sensors were mapped and spatially joined to this 6 km grid (for VIIRS EDR and GOCI products) or 3 km grid (for VIIRS IP and MODIS C6 3 km products) to construct coincident satellite-ground AOD pairs.

To assess the intra-city spatial variations of aerosol loadings, we analyzed ground AOD observations over Beijing, Osaka, and Seoul from handheld sunphotometer and DRAGON-Asia stations in 2012. First, the great circle distance between each of two ground observation sites which are less than 20 km apart were calculated. Then we stratified the site-to-site distances by increments of 750 m, the resolution of VIIRS IP aerosol product, and calculated the station-to-station correlation coefficients of daily average AOD within each distance stratum. The observations from DRAGON sites in Osaka and Seoul and from handheld sunphotometers in Beijing were processed separately due to differences in instrumentation. Only handheld sunphotometer AOD observations in Beijing from 15 February 2012 to 31 May 2012 were included to ensure that the study period at these three locations is the same.

To validate the performance of high-resolution satellite aerosol products, two types of comparisons were conducted: the temporal comparison, which compared satellite AOD retrievals within  $3 \times 3$  grid cells sampling buffers against ground AOD from AERONET stations during 1 year from July 2012 to June 2013; and the spatial comparison, which compared satellite AOD retrievals within single grid cell sampling buffers against spatially concentrated ground AOD from DRAGON stations or the handheld sunphotometer. Temporal comparisons and spatial comparisons differ in study periods (Table 2): the temporal comparison period was the longest overlap period covered by all five satellite products and the spatial comparison periods in Beijing and the Japan–South Korea region are different in order to include the maximum number of ground observations. The coefficients of variation (CV), which is standard deviation divided by mean of AOD retrievals, from various sensors in temporal-comparison sampling buffers were calculated and reported below to assess the homogeneity of aerosol loading within buffers. The mean CV from various aerosol products ranged between 0.18 and 0.35, indicating that, as expected, certain heterogeneity in aerosol loading existed within the

**Table 1.** Characteristics and quality control criteria of satellite aerosol products.

Data set	Including criteria	Resolution	Coverage
VIIRS EDR	Quality Flag = High	6 km, daily	Global
VIIRS IP	Quality Flag = High	0.75 km, daily	Global
GOCI	Quality Flag = 3	6 km, 8-hourly obs. per day	East Asia
Aqua MODIS C6 3 km	Quality Flag = 3	3 km, daily	Global
Terra MODIS C6 3 km	Quality Flag = 3	3 km, daily	Global

**Table 2.** Characteristics of ground AOD measurement data sets.

		Temporal comparison	Spatial comparison
Beijing	Data set	AERONET	Microtops II
	Including criteria	Level 1.5	Median/SD < 2
	Study period	Jul 2012–Jun 2013	Jan 2012–Jun 2013
East Asia	Data set	AERONET	DRAGON
	Including criteria	Level 2.0	Level 2.0
	Study period	Jul 2012–Jun 2013	15 Feb–31 May 2012

temporal-comparison buffer. This relatively small heterogeneity should not be a detriment to the temporal comparison; however, some extremely large CV values that were probably due to very small mean AOD values were observed. In order to avoid potentially large variations in aerosol loading within buffers, we removed satellite pixels with CVs outside the range of  $\pm 1.0$  (Liu et al., 2007) in temporal comparisons. Moreover, the existing heterogeneity of AOD loading encouraged us to conduct spatial comparisons implementing smaller sampling buffers.

For the temporal comparison of VIIRS EDR data, we averaged valid AOD retrievals in each  $3 \times 3$  grid cells sampling buffer ( $18 \times 18 \text{ km}^2$ ) centered at each ground AERONET station. The mean and median CV were 0.25 and 0.21, respectively. The average AOD values were then compared with the mean AERONET AOD within a 1 h time window ( $\pm 30$  min around the satellite overpass time). We employed this smaller spatial averaging window than the widely used 27.5 km radius circle buffer suggested by the Multi-sensor Aerosol Products Sampling System (MAPSS) (Seo et al., 2015) in order to examine the performance of these finer resolution products at the scale of their expected application conditions. We used the typical 1 h time window because a previous analysis indicated that changing the time window matters little to validation results (Remer et al., 2013) and the 1 h time window yields a larger database for the validation. For the spatial comparison of VIIRS EDR data, we used single 6 km pixels covering each ground observation location, i.e. DRAGON station or handheld sunphotometer measurement location, and compared the AOD retrieval values with the mean AOD from the corresponding DRAGON sta-

tion within the 1 h time window or the median AOD from the handheld sunphotometer at the corresponding location. The temporal and spatial comparisons of GOCI data followed the same protocol as described above. Although GOCI provides eight hourly AOD retrievals per day, we only used retrievals at 1:00 pm LT in the comparison in order to make the validation results comparable among these satellite products. The mean and median CV of GOCI retrievals within the  $3 \times 3$  grid cells sampling buffer were 0.35 and 0.15, respectively.

For the comparisons of VIIRS IP data, we used the 3 km grid because we did not have enough ground sampling data to create a 750 m grid. For the temporal comparison, we averaged valid IP AOD retrievals falling in the 3 km grid cell centered at each ground AERONET station and the mean and median CV were 0.33 and 0.25, respectively, within the 3 km grid cell buffer. This sampling buffer roughly covered a  $4 \times 4$  pixel group. The average AOD values were compared against average AOD from the corresponding AERONET station within the 1 h time window. In the spatial comparison of VIIRS IP, we also used the 3 km sampling buffer due to a lack of more spatially concentrated ground AOD observations. Thus, the VIIRS IP data are oversampled in the spatial comparison. For the temporal comparison of Aqua and Terra MODIS C6 3 km data, we employed the 3 km grid and averaged valid AOD retrievals in each  $3 \times 3$  grid cells centered at each ground AERONET station to compare with the mean AOD within the 1 h time window. The mean CV of Aqua and Terra MODIS within the  $3 \times 3$  grid cells sampling buffer were 0.18 and 0.13, respectively. For the spatial comparison of MODIS C6 3 km data, we used the individual 3 km pixel AOD value falling on each ground observation loca-

tion to compare with average AOD from the corresponding DRAGON station within the 1 h time window or the median AOD from the handheld sunphotometer at the corresponding location.

In summary, coincident satellite–ground AOD pairs were defined as average satellite AOD retrievals within the specific sampling buffer matched with average ground AOD observations of the corresponding site within 1 h time windows with respect to satellite pass over time. For VIIRS EDR and GOCI products, the temporal and spatial comparison buffer was  $18 \times 18 \text{ km}^2$  and  $6 \times 6 \text{ km}^2$ , respectively. For the VIIRS IP product, the temporal and spatial comparison employed the same  $3 \times 3 \text{ km}^2$  buffer. For MODIS C6 3 km product, the temporal and spatial comparison buffer was  $9 \times 9 \text{ km}^2$  and  $3 \times 3 \text{ km}^2$ , respectively. The examples of buffers used in the temporal and spatial comparisons for each satellite product are shown in the Supplement (Fig. S1). It is notable that both MODIS and VIIRS pixels were stretched toward the edge of the scan. For example, the  $3 \times 3 \text{ km}^2$  MODIS pixels become approximately  $6 \times 12 \text{ km}^2$  toward the edge. Thus, the spatial joining and our construction of coincident satellite–ground AOD pairs may slightly decrease the coverage for MODIS and VIIRS products and may potentially affect the spatial comparison results.

In epidemiological studies, in order to improve the coverage of satellite aerosol data to provide exposure assessment, spatial aggregation is widely used. In our analysis, we constructed quality flags for each satellite–ground AOD collection to obtain better coverage without losing accuracy. For the temporal validation, coincident satellite–ground AOD pairs with at least 20 % coverage of both satellite data and ground data (Levy et al., 2013) (e.g., having two or more satellite pixels within the sampling buffer and at least two AERONET/DRAGON AOD within the 1 h time window) were marked as “High Quality”; coincident satellite–ground AOD pairs with less than 20 % satellite pixels falling in the sampling buffer but one or more pixels located within the grid cell centered on the ground stations were marked as “Medium Quality”; all other coincident satellite–ground AOD pairs were marked as “Low Quality”. Since we did not create a 750 m grid for the VIIRS IP product, VIIRS IP–ground AOD pairs were assigned either “High Quality” or “Low Quality”. In the spatial validation, because the best scenario satellite–ground AOD collection is to have one or more satellite pixels within the one-grid cell sampling buffer and two or more AERONET/DRAGON AOD during the 1-hour time window, we only assigned two quality levels: “High Quality” for coincident satellite–ground AOD pairs in the best scenario, and “Low Quality” for all others. Only coincident satellite–ground AOD pairs with high and medium quality were included in our validations. We also conducted a comparison, shown as Table S3 in the Supplement, including all the satellite–ground AOD pairs—regardless of their quality—to examine the influence of sampling bias. In addition, we conducted sensitivity analyses on VIIRS IP AOD re-

trievals including both high- and degraded-quality retrievals (Table S2) and for the GOCI product at an hourly scale (Table S5) with respect to its eight hourly observations per day. In the hourly comparison, we constructed hourly average AERONET AOD as the ground true value and employed the same  $3 \times 3$  grid cells temporal comparison sampling buffer.

## 2.5 Evaluation metrics

Several metrics were used to evaluate the performance of satellite aerosol products in this study. Coverage (%) describes the availability of site–day (or site–hour for GOCI data) satellite retrievals when the ground AERONET AOD were available in the temporal comparison. We include all available matched satellite retrievals when calculating the coverage regardless of the quality flag of the coincident satellite–ground AOD pairs. Pearson correlation coefficient describes the correlation between satellite retrievals and ground AOD. Bias describes the average difference between satellite retrievals and ground AOD. We calculated the percent of retrievals falling within the expected error (EE) range. For the consistency of the last metric among different aerosol products, we employed the same EE,  $\pm(0.05 + 0.15 \text{ AOD})$ , which is established during the global validation of MODIS C5 aerosol product over land, in this study. In addition, linear regression with satellite retrievals as the dependent variable and ground AOD as the independent variable was employed. The slopes and intercepts from linear regressions were reported. The residuals of the linear regressions were slightly skewed (Table S1), indicating that one assumption of linear regression, normality of the residual distribution, was not fully met. However, log-transformation did not necessarily make the residual distribution more normal (Table S1) and log-transformation led to loss of physical meaning of evaluation metrics as well as making the evaluation metrics incomparable to previous studies. All things considered, we used the original data in this analysis. We conducted a sensitivity analysis using log-transformed data after adding 0.05 to GOCI, Aqua and Terra MODIS C6 3 km satellite retrievals as well as corresponding AERONET retrievals over Japan–South Korea region.

## 3 Results and discussion

### 3.1 Spatial variations of aerosol loadings

Figure 2a shows the correlation coefficient of daily AOD by binned distance and Fig. 2b shows the site-specific average AOD with the regional average AOD subtracted in these three cities. Figure 2a indicates that the DRAGON AOD were highly correlated within a 20 km spatial range with a correlation coefficient larger than 0.9. However, results from handheld sunphotometer observations in Beijing suggest that the spatial correlation coefficients declined slowly as the distance between two measurement locations increased up to

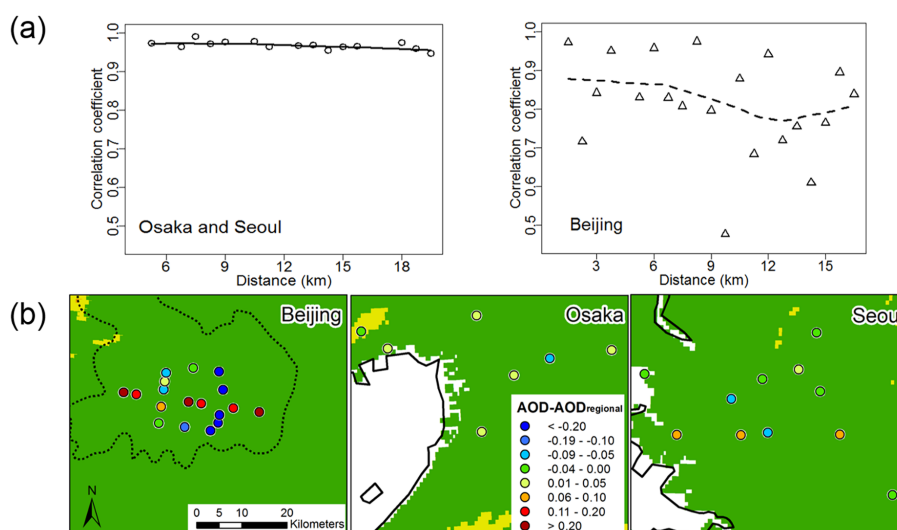


**Figure 2.** (a) The station to station correlation coefficients of daily mean AOD stratified by distance over (left) DRAGON-Asia region (right) Beijing region. The line is the Loess curvy. (b) The spatial distribution of average AOD in these three cities. The background color shows the elevation with the same color scale as in Fig. 1.

12 km. The correlation coefficient increased slightly when the distance among two measurement locations are beyond 12 km. This can be explained by the clustered distribution of ground measurement locations in Beijing: these long location-to-location distances only occur when the two locations are located along the Chang’an Avenue and, since vehicle exhaust is one of the major sources of aerosol in Beijing, these AOD are highly correlated. The different aerosol spatial variability trends in Beijing and in the DRAGON domain can be attributed to the following reason: first, the DRAGON-Asia campaign provides real-time observation but our ground AOD observations in Beijing provide one observation at each site per day, so that the average daily AOD from DRAGON stations may have smoothed away some of the spatial heterogeneity. Second, the handheld sunphotometer may introduce larger measurement errors than DRAGON stations, due to both instrument quality and operation errors. Previous evaluation indicates that handheld stability and inaccurate pointing to the Sun significantly affects the accuracy of measurements by Microtops II (Ichoku et al., 2002; Morys et al., 2001). Our comparison of Microtops II AOD with nearby AERONET data yielded a slope of  $\sim 0.95$ , a correlation coefficient of  $\sim 0.8$ , and an intercept of 0.16 (Text S1), indicating that the handheld sunphotometer AOD are usable.

Even though the aerosol loadings are highly related spatially, the AOD value may differ among nearby stations (Fig. 2b). In Beijing, the difference in average AOD between two neighboring sites that are  $\sim 6$  km apart can be as high as 0.4, about 49 % of the regional mean AOD value. The observations from DRAGON stations show smaller differences in average AOD relative to those in Beijing, but the difference between two neighboring sites can still be greater than

0.1 in Seoul: 23 % of the regional mean AOD value. These results indicate that spatial contrast in aerosol loading exists at local scale and finer resolution satellite aerosol products are needed to better characterize individual and population exposure of particulate pollution.

### 3.2 The Beijing sampling experiment

The GOCI aerosol product provided the highest coverage in the temporal comparison over Beijing with 73 % available retrievals relative to AERONET AOD within the 1 h time window ( $\pm 30$  min around the satellite overpass time), followed by the VIIRS IP (42 %), VIIRS EDR (41 %), MODIS Terra C6 3 km product (40 %), and MODIS Aqua C6 3 km product (38 %) (Table S2). Table 3 shows the statistical metrics from the temporal and spatial comparisons over Beijing. In the temporal comparison, the GOCI product provided the most accurate AOD retrievals, which slightly overestimated AOD by 0.02 on average. Other aerosol products significantly overestimated AOD with the average bias in the temporal comparison for VIIRS EDR, VIIRS IP, Aqua and Terra MODIS C6 3 km products equal to 0.11, 0.25, 0.21, and 0.29, respectively. Though GOCI AOD retrievals agreed well with ground AOD in the temporal comparison, with 55 % of GOCI AOD retrievals at 13:00 falling within the EE, only 37 % of GOCI AOD retrievals fell within the EE in the spatial comparison. The comparison including all eight hourly GOCI observations represented reduced coverage (59 %), a smaller average bias ( $-0.006$ ), and a larger proportion of retrievals fell within EE (59 %). Thus, the GOCI product resolved the temporal and spatial variability of aerosol loadings at its designed temporal and spatial resolutions, but it tracked

**Table 3.** Statistics of the temporal and spatial comparisons between satellite retrievals and ground AOD measurements at 550 nm in Beijing.

	<i>N</i>	<i>R</i> <sup>2</sup>	Slope	Intercept	Bias	%EE
Temporal comparison						
VIIRS EDR	90	0.70	0.96	0.12*	0.11	52
VIIRS IP	133	0.63	1.00	0.25*	0.25	32
GOCI	142	0.88	0.95	0.05	0.02	55
GOCI all obs.	957	0.88	0.98	0.008	−0.006	59
Aqua MODIS C6 3 km	119	0.81	1.05	0.19*	0.21	44
Terra MODIS C6 3 km	133	0.80	0.99	0.30*	0.29	25
Spatial comparison						
VIIRS EDR	108	0.14	0.25	0.34*	0.04	51
VIIRS IP	150	0.16	0.34	0.45*	0.18	33
GOCI	124	0.51	0.74	0.23*	0.00	37
Aqua MODIS C6 3 km	77	0.68	1.19	0.22*	0.31	16
Terra MODIS C6 3 km	73	0.85	1.00	0.30*	0.30	26

\* *p* value < 0.01. All the slopes are statistically significant with *p* value < 0.01.

the small-scale spatial variability less well than the temporal variability in Beijing.

VIIRS EDR product performed well in Beijing in both the temporal and spatial comparisons, with 52 and 51 % of retrievals falling within the EE in the temporal and spatial comparison, respectively. Although VIIRS IP had a relatively large positive bias (0.25) in the temporal comparison, it provided acceptable coverage with 33 % retrievals falling within the EE in the spatial comparison, resolving valuable information of small-scale aerosol variability in urban areas. The MODIS C6 3 km product had the largest high bias and lowest % EE in this spatial comparison, with 16 and 26 % of retrievals falling within the EE for Aqua and Terra MODIS, respectively. A previous validation study of the 3 km MODIS AOD data also reported similar retrieval errors in urban areas (Remer et al., 2013). It is notable that the *R*<sup>2</sup> values of the MODIS C6 3 km products is the highest in the spatial comparisons (0.68 for Aqua and 0.85 for Terra) and the linear regression statistics indicates that the low percent of retrievals falling within EE is mainly due to a relatively constant positive offset: the intercepts for Aqua and Terra are 0.22 and 0.30, respectively. One possible explanation of the positive bias of MODIS and VIIRS products is that our study domain is highly urbanized with bright surfaces, and therefore is challenging for the Dark Target algorithm.

### 3.3 The temporal evaluation of AOD over the Japan–South Korea region

We first looked at the AOD retrievals distribution on one clear day, 7 May 2012, during the DRAGON period (Fig. 3). Figure 3 indicates that the sampling strategies and cloud masks differ in these five satellite aerosol products, resulting in different patterns of missing data. GOCI provided the best coverage with almost no missing data over this region. VIIRS

products and MODIS products showed similar missing data in the center of the map but were less consistent at its edges; while VIIRS products showed more missing data in the lower right corner, MODIS products showed more missing in the upper right corner. VIIRS and MODIS pixels are stretched toward the edge of the scan. VIIRS and MODIS products tended to overestimate AOD values in the urban area (Seoul), but GOCI provided accurate AOD estimates in this region. Though these 3 km products showed similar spatial distribution patterns to the 6 km products, the 3 km products demonstrated greater heterogeneity, which is valuable to analyze local aerosol sources and estimate personal air pollution exposure.

Similar to the comparisons in Beijing, the GOCI aerosol products provided the highest coverage in the temporal comparison over the Japan–South Korea region, with 74 % retrievals relative to AERONET observations within the 1 h time window ( $\pm 30$  min around the satellite overpass time), followed by VIIRS EDR (63 %), VIIRS IP (50 %), Terra MODIS C6 3 km (26 %), and Aqua MODIS C6 3 km (24 %) (Table S2). It is notable that the seasonal missing pattern due to cloud cover and weather conditions may vary across these satellite aerosol products. However, since we did not have enough coincident satellite-ground AOD pairs to conduct seasonal evaluation, the seasonal missing patterns and seasonal performance of these satellite aerosol products were not analyzed in this study. The distributions of the coincident satellite-AERONET AOD pairs with high or medium quality are shown in Fig. 4. The distribution of the Terra MODIS C6 product is not shown here because it passes the study region in the morning, leading to potential differences in AOD distribution relative to other sensors that pass the study region in the afternoon. This histogram is plotted with frequency of AOD retrievals from each sensor relative to the total number



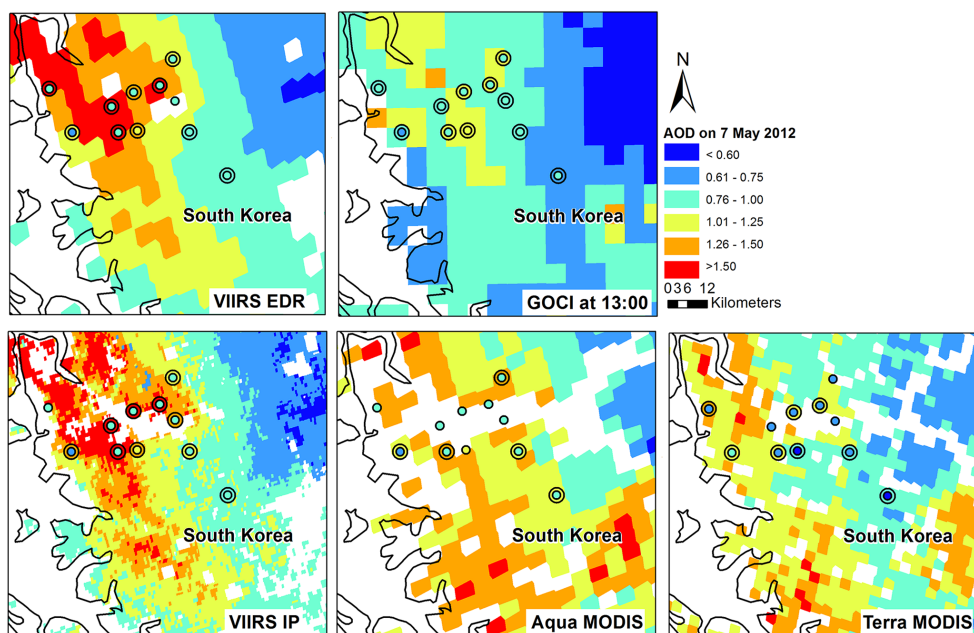


**Figure 3.** The AOD retrievals at 550 nm from different satellite aerosol products at their designed resolution on 7 May 2012. Coincident Satellite-DRAGON AOD pairs are shown in double circles: the inner circle is the average DRAGON observation within  $\pm 30$  min of satellite overpass and the outer circle is the satellite retrieval that the DRAGON stations falls in.

of matched AOD retrievals from the corresponding sensor rather than the count of AOD retrievals because these aerosol products differ in sampling strategies, leading to different total number of coincident satellite-ground AOD pairs. VIIRS EDR, VIIRS IP, and GOCI products showed a similar mode of distribution to AERONET AOD, with the peak probability around 0.2. The distribution of Aqua MODIS C6 3 km AOD had the peak around 0.3, indicating that the Aqua MODIS C6 3 km product tended to overestimate AOD in general. A previous study also reported that the MODIS C6 3 km product had a decreased proportion of low AOD values and an increased proportion of high AOD values (Remer et al., 2013) relative to the 10 km product over land, leading to a higher global average AOD. The VIIRS IP product also tended to overestimate AOD, with higher percentage of retrievals occurring at high AOD values. The distribution of GOCI data provided the best fit with AERONET data, with a correlation coefficient of 0.95, followed by VIIRS EDR ( $R^2 = 0.93$ ), VIIRS IP ( $R^2 = 0.77$ ), and MODIS Aqua C6 3 km product ( $R^2 = 0.76$ ). The difference in the distributions of these satellite aerosol products can be partly explained by different retrieval assumptions including aerosol models, different surface reflectance and different global sampling strategies. Moreover, these satellite aerosol products differ in the valid AOD retrieval ranges, leading to differences in the distribution of extremely high and low AOD values.

The temporal comparisons over the Japan–South Korea region showed more retrievals falling within the EE and smaller biases relative to comparisons in Beijing. Figure 5

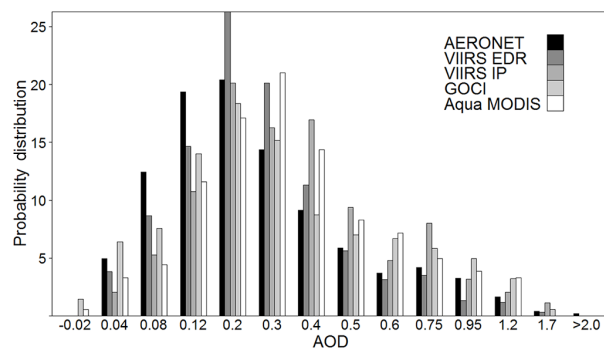


**Figure 4.** Histogram for the matched satellite AOD retrievals and AERONET measurements. The  $x$  axis shows AOD values and the  $y$  axis shows the frequency of AOD observations from each sensor relative to the total number of matched AOD observations from the corresponding sensor.

shows the frequency scatter plots showing the results of temporal comparisons over the Japan–South Korea region and the corresponding box plots showing the difference between satellite AOD retrievals and ground observations. GOCI retrievals at 13:00 LT were highly correlated with the ground AOD with an  $R^2$  of 0.80. The linear regression of GOCI retrievals and ground AOD fell close to the 1:1 line with a small offset (0.04), and 61 % of GOCI retrievals at 13:00 LT fell in the EE. Comparison including eight GOCI hourly retrievals showed a higher  $R^2$  of 0.82 with a smaller average bias (0.02), with 66 % of retrievals falling within the EE (Ta-

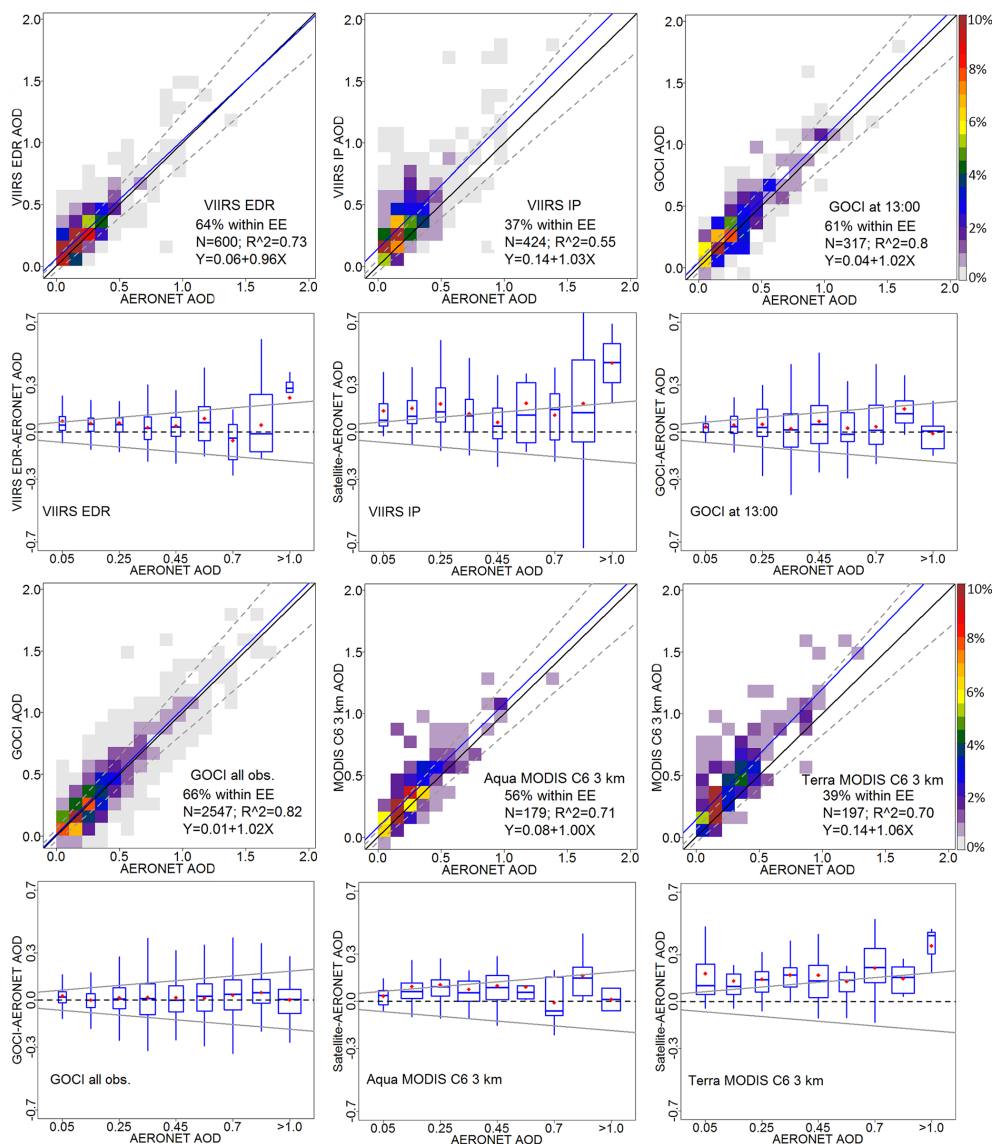


**Figure 5.** First and third rows: frequency scatter plots of satellite AOD retrievals against AERONET AOD measurements at 550 nm over the Japan–South Korea region. The linear regression is shown as solid blue line and all the linear relationships are statistically significant at the alpha level of 0.01. The boundary lines of the expected error are shown in the dash lines, and the one-one line is shown as solid black lines for reference. Second and fourth rows: box plots of AOD errors (satellite – AERONET) versus AERONET AOD over the Japan–South Korea region. The one-one line (zero error) is shown as a dash line and the boundary lines of the expected error are shown as gray solid lines. For each box-whisker, its properties and representing statistics include the following: width is  $\sigma$  of the satellite AOD; height is the interquartile range of AOD error; whisker is the  $2\sigma$  of the AOD error; middle line is the median of the AOD error; and red dot is the mean of the AOD error.

ble 4, GOCI all obs.). The box plot indicates that GOCI retrievals overestimated AOD at high AOD values ( $\text{AOD} > 0.6$ ) (Fig. 5). Thus, the GOCI product tracked the daily variability of aerosol loadings well and it provided additional information to study short-term aerosol trends. Similarly, 64% of VIIRS EDR retrievals fell into the EE with a slightly higher bias (0.05) and a slightly lower  $R^2$  of 0.73 (Table 4). This positive bias is consistent with a previous global validation study, which reports a 0.01 bias of VIIRS EDR in East Asia

(Liu et al., 2014). Though the VIIRS EDR product tended to overestimate AOD at low ( $\text{AOD} < 0.3$ ) and high AOD values ( $\text{AOD} > 1.0$ ), it agreed well with the AERONET observations when AOD ranged between 0.3 and 1.0 (Fig. 6).

The VIIRS IP had a linear regression slope close to 1 (1.03) against AERONET observations, but it had a consistent positive bias of 0.15 on average. Only 37% of VIIRS IP retrievals fell within the EE. The scatter plot indicates that the IP retrievals varied substantially, especially when the

**Table 4.** Statistics of the temporal and spatial comparisons between satellite retrievals and ground AOD measurements at 550 nm over Japan–South Korea region.

	<i>N</i>	<i>R</i> <sup>2</sup>	Slope	Intercept	Bias	%EE
Temporal Comparison						
VIIRS EDR	600	0.74	0.96	0.06 <sup>b</sup>	0.05	64
VIIRS IP	424	0.55	1.03	0.14 <sup>b</sup>	0.15	37
GOCI	317	0.80	1.02	0.04 <sup>b</sup>	0.05	61
GOCI all obs.	2547	0.82	1.02	0.01 <sup>a</sup>	0.02	66
Aqua MODIS C6 3 km	179	0.71	1.00	0.08 <sup>b</sup>	0.08	56
Terra MODIS C6 3 km	197	0.70	1.06	0.14 <sup>b</sup>	0.16	39
Spatial Comparison						
VIIRS EDR	144	0.53	0.96	0.18 <sup>b</sup>	0.16	41
VIIRS IP	229	0.60	1.11	0.21 <sup>b</sup>	0.26	26
GOCI	196	0.79	1.19	−0.09 <sup>b</sup>	0.03	48
Aqua MODIS C6 3 km	108	0.81	1.26	0.07 <sup>a</sup>	0.19	28
Terra MODIS C6 3 km	132	0.73	1.00	0.23 <sup>b</sup>	0.23	27

<sup>a</sup> *p* value < 0.05. <sup>b</sup> *p* value < 0.01. All the slopes are statistically significant with *p* value < 0.01.

AOD values were low. MODIS C6 3 km products had a high positive bias of 0.08 for Aqua and 0.16 for Terra. Consistent with what was reported by a previous global evaluation study, we observed that the MODIS C6 3 km products tended to overestimate AOD and the bias increased with AOD values (Remer et al., 2013). 56 % of the Aqua MODIS C6 3 km retrievals and 39 % of the Terra MODIS C6 3 km retrievals fell within the EE. In general, these finer resolution aerosol products included larger bias relative to lower resolution products and researchers must be cautious when applying them by, for example, calibrating these high-resolution satellite aerosol products in specified study regions and implementing appropriate data filtering strategies.

Since the GOCI product provides eight hourly observations per day, to examine the temporal variability in the accuracy of GOCI aerosol retrievals, we compared the GOCI AOD retrievals with AERONET AOD stratified by hour (Table S5). In general, the GOCI product provided high-quality retrievals consistently throughout the day except that it tended to slightly overestimate AOD in the morning and underestimate AOD in the afternoon. Such temporal variability in accuracy was also reported by a previous evaluation study of the Geostationary Operational Environmental Satellite (GOES) aerosol product (Morys et al., 2001). The daily variability in the quality of GOCI retrievals may be due to changes in scattering angle, clouds, and the associated Bidirectional Reflectance Distribution Function (BRDF) effects.

Ten-fold cross validation was conducted for the comparison of VIIRS and GOCI products to detect overfitting. The linear regression statistics of cross validation did not change significantly relative to the statistics of comparisons. The cross validation *R*<sup>2</sup> values of VIIRS EDR, VIIRS IP, GOCI at 13:00, and GOCI 8 observations data were 0.73, 0.51, 0.78,

and 0.82, respectively. In addition, to detect the spatial variability of the satellite retrieval performance, we applied the regionally developed linear regression parameters of GOCI 8 observations data to individual AERONET station in the Japan–South Korea region. The linear regressions with the satellite AOD as the dependent variable and the fitted AOD from a regional model as the independent variable yielded *R*<sup>2</sup> larger than 0.75 at all sites except the AERONET sites “Nara” and “Osaka”, two stations located in Osaka. This result indicated that parameters from the regional data set were valid locally. Limited by sample size, we did not apply this method to other aerosol products.

### 3.4 The spatial evaluation of AOD over the Japan–South Korea region

The mean daily AOD from different sensors and AERONET stations during the 1-year period from July 2012 to June 2013 are shown in Fig. 6. These five aerosol products provided similar distributions of average AOD during the 1-year period, with the highest values occurring in northeastern China and the Yangtze River delta, and the lowest values occurring in southern China and Japan. Several high-AOD-value spots appeared along the west coast of South Korea and surrounded the Seto Inland Sea, likely due to emissions from urban centers in these regions. These five maps differ in missing patterns due to their different masking approaches. The VIIRS algorithms did not retrieve AOD over inland lakes (e.g. the Taihu Lake); the GOCI product retrieved AOD over inland water; while MODIS products provided some AOD retrievals over inland lakes, with some missing data. The GOCI product did not provide high-quality retrievals at some locations in central Japan due

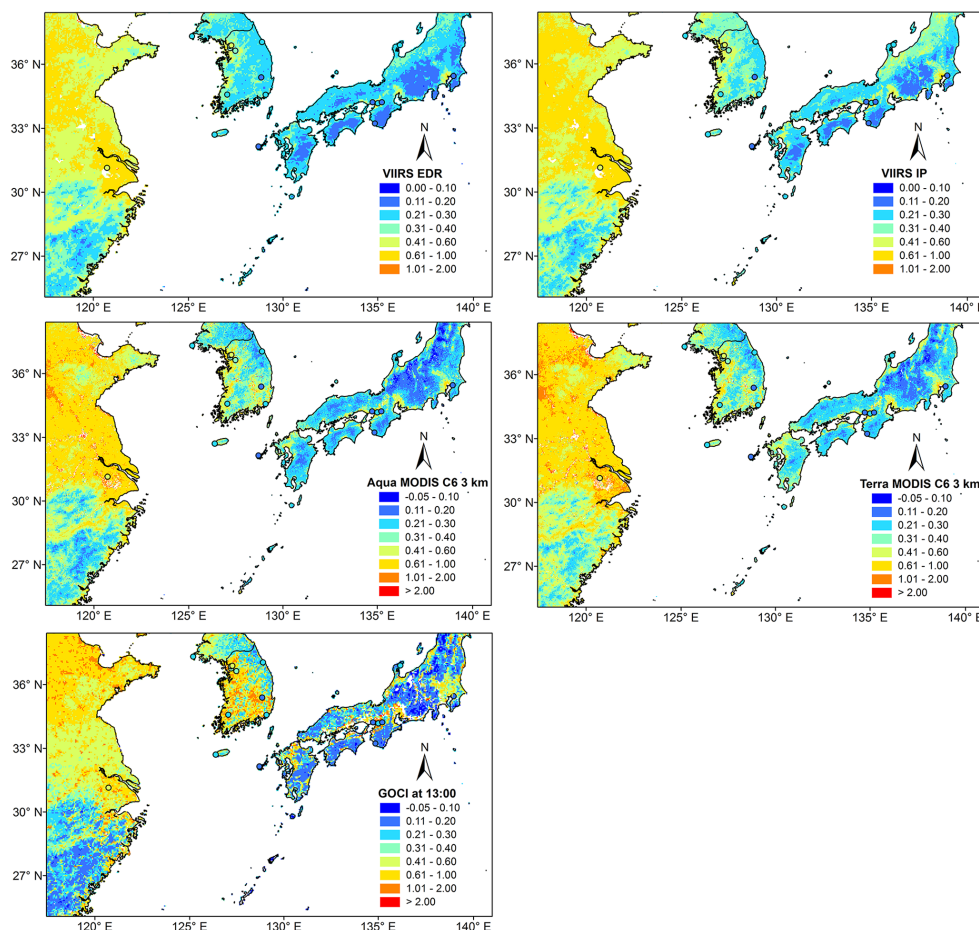


**Figure 6.** The distributions of the 12 months average AOD values from July 2012 to June 2013 from VIIRS EDR, VIIRS IP, Aqua MODIS C6 3 km, Terra MODIS C6 3 km, and GOCI data sets.

to snow coverage in this mountain region. To maintain a consistent evaluative data filtering strategy, the inland water AOD retrievals and ground observations were removed from the validation. The VIIRS EDR product showed lower AOD values in northeastern China and South Korea relative to AOD retrievals from other sensors. The VIIRS IP product also showed lower AOD values in northeastern China, but provided higher AOD retrievals in northern Japan. This can be explained by the system bias reported in a previous study that VIIRS retrievals tend to underestimate AOD when NDVI value is low and overestimate AOD over vegetated surfaces (Liu et al., 2014). The VIIRS IP product had higher AOD values relative to the EDR product, especially over the Korean Peninsula and northern Japan. This may be due to IP's ability to track small-scale variability which were smoothed in the EDR retrievals, or may result from the positive bias of IP observed in the temporal comparison. Because VIIRS aerosol products restrict valid AOD values to between 0.0 and 2.0, they may underestimate AOD values when the aerosol loadings are extremely high, like in northeastern China, though we lacked ground AOD data in this region

to test this hypothesis. Aqua and Terra MODIS C6 3 km aerosol products showed similar spatial distribution in AOD retrievals, with higher AOD values in urban areas (e.g., over the Yangtze River Delta and North China Plain in China). GOCI presented some high AOD values in local regions such as western South Korea, around the Seto Inland Sea, and over northeastern China. However, it showed lower AOD values over the Yangtze River Delta in China. This result is consistent with the temporal comparison results shown in Fig. 5 that the GOCI product slightly overestimated AOD at high AOD values ( $AOD > 0.6$ ). Compared with ground AOD, all these five aerosol products overestimated AOD in Japan, where the average AOD values were relatively low. VIIRS EDR tended to slightly underestimate AOD over the Seoul region. The lack of ground AOD, especially in northeast China, makes it impossible to quantitatively evaluate the spatial distribution of these aerosol products in China.

Results of the spatial comparison over DRAGON-Asia region are shown in Table 4. Satellite aerosol products performed better in tracking the day-to-day variability relative to tracking their spatial patterns. In the spatial comparison,

all the satellite aerosol products showed lower  $R^2$  and larger offset with less retrievals falling into the EE. GOCI product provided the highest accuracy, with a small positive bias of 0.03 and 48 % of retrievals falling in the EE, followed by VIIRS EDR, with a positive offset of 0.16 and 41 % of retrievals falling in the EE. In contrast, VIIRS IP and MODIS C6 3 km had large positive biases, and less than 30 % of retrievals fell within the EE due to larger noise (related to the finer resolutions). There is evidence that this positive bias includes systematic errors due to improper characterization of surface reflectance, uncertainties in the assumed aerosol model, and cloud masking. The 3 km MODIS products sample fewer reflectance pixels to retrieve aerosol pixels relative to the 10 km products, introducing sporadic unrealistic high AOD retrievals that are avoided more successfully by the 10 km products (Munchak et al., 2013). Previous studies also reported that improper characterization of bright urban surfaces, a known difficult situation for the Dark Target algorithm, led to positive bias in urban and suburban regions (Munchak et al., 2013; Remer et al., 2013). The VIIRS IP product is retrieved at the reflectance pixel level without aggregation, thus it is expected to include more noise. Though these finer resolution aerosol products did not fully track the spatial trends of aerosol loading at their designed resolution, they provide additional information about aerosol spatial distribution and will benefit exposure assessments at local scales.

To examine possible sampling bias due to our data inclusion criteria, we performed temporal and spatial comparisons including all the coincident satellite-ground AOD pairs over the Japan–South Korea region (Table S3). There is no significant change in the evaluation metrics after including pairs with low quality. Thus, the validation results are robust and there is no evidence for sampling bias. We validated the VIIRS IP AOD retrievals with degraded quality over the Japan–South Korea region and observed lower correlation coefficients, higher biases, and less retrievals falling within the EE in both the temporal and spatial comparisons (Table S4). This result suggests to use only high-quality VIIRS IP retrievals. We also validated the GOCI AOD retrievals with different quality over the Japan–South Korea region. Including medium- and low-quality GOCI retrievals decreased the accuracy, but significantly increased the coverage (Table S6). By including the retrievals having quality flags equal to both 3 and 2, the coverage increased from 27 to 38 % in the temporal comparison over the Japan–South Korea region, while the average bias increased by 0.01 and the percentage of retrievals falling within the EE decreased by 7 %. Thus, including retrievals with medium quality might be acceptable, depending on study objectives. Results from linear regressions with log-transformed data (Table S7) indicated that GOCI aerosol products provided the best estimate of ground-measured AOD, followed by VIIRS EDR and MODIS Aqua C6 3 km products. Due to the relatively small number of matched observations, analysis of the correlation between

quality of satellite aerosol retrievals and satellite viewing angles were beyond the scope of this analysis. However, previous studies reported that towards the edge of the scan, VIIRS EDR tends to underestimate AOD over land (Liu et al., 2014).

#### 4 Conclusion

In this work, the intra-city variability of aerosol loadings were examined with ground AOD from the DRAGON-Asia campaign and our mobile sampling campaign in Beijing. Five emerging high-resolution satellite aerosol products are evaluated by comparing them with ground AOD from AERONET, DRAGON, and handheld sunphotometers over East Asia in 2012 and 2013. We observed variability in both correlation coefficients and average AOD values among ground AOD observation sites in three urban centers in Asia. Evaluation results indicated (a) that the 6 km resolution products – VIIRS EDR and GOCI – provided more accurate retrievals with higher coverage relative to the higher resolution products – VIIRS IP, Terra and Aqua MODIS C6 3 km products – in both temporal comparisons and spatial comparisons; however, VIIRS IP and MODIS C6 3 km products provide additional information about fine-resolution aerosol spatial distribution and will benefit exposure assessments at local scales; (b) satellite aerosol products resolved the day-to-day aerosol loading variability better than the spatial aerosol loading variability; and (c) satellite products performed less well in Beijing relative to the Japan–South Korea region, indicating that retrieval in urban areas is challenging. These satellite aerosol products have their own advantages and disadvantages. For example, the GOCI aerosol product provides high-accuracy AOD retrievals eight times per day, but it only covers East Asia; the VIIRS EDR product provides high-accuracy AOD retrievals and global coverage once per day, but its 6 km resolution is relatively low; the MODIS C6 3 km products provide high-resolution AOD retrievals with global coverage, but have positive bias in urban regions. Researchers need to apply these aerosol products according to specified research objectives and study design. The performance of these aerosol products over Beijing and the Japan–South Korea region demonstrates that satellite aerosol products can track the small-scale variability of aerosol loadings. High-resolution satellite aerosol products provide valuable information for the spatial and temporal characterization of  $PM_{2.5}$  at local scales. Future studies with additional ground AOD observations at fine spatial and temporal scale will help us analyze air pollution patterns and further validate satellite products.

**The Supplement related to this article is available online at doi:10.5194/acp-16-1255-2016-supplement.**

**Acknowledgements.** The work of Y. Liu and Q. Xiao was partially supported by the NASA Applied Sciences Program (grants NNX11AI53G and NNX14AG01G, PI: Liu). We would like to acknowledge the AERONET team, I. Sano and the DRAGON-Japan team, the Yonsi team and their collaborators in S. Korea, and CARSONET and CAS teams in and around Beijing for providing data support in this study. The AERONET project was supported by the NASA EOS project office, and by Hal B. Maring, Radiation Sciences Program, NASA Headquarters. This research was a part of the project titled “Research for Applications of Geostationary Ocean Color Imager”, funded by the Ministry of Oceans and Fisheries, Korea. The MODIS project was supported by the NASA Earth Science Program, grant NNH13ZDA001N-TERAQEA.

Edited by: Y. Rudich

## References

- Anderson, T. L., Charlson, R. J., Winker, D. M., Ogren, J. A., and Holmén, K.: Mesoscale Variations of Tropospheric Aerosols, *J. Atmos. Sci.*, 60, 119–136, 2003.
- Choi, M., Kim, J., Lee, J., Kim, M., Je Park, Y., Jeong, U., Kim, W., Holben, B., Eck, T. F., Lim, J. H., and Song, C. K.: GOCI Yonsei Aerosol Retrieval (YAER) algorithm and validation during DRAGON-NE Asia 2012 campaign, *Atmos. Meas. Tech. Discuss.*, 8, 9565–9609, doi:10.5194/amt-d-8-9565-2015, 2015.
- Evans, J., van Donkelaar, A., Martin, R. V., Burnett, R., Rainham, D. G., Birkett, N. J., and Krewski, D.: Estimates of global mortality attributable to particulate air pollution using satellite imagery, *Environ. Res.*, 120, 33–42, 2013.
- Holben, B., Eck, T., Slutsker, I., Tanre, D., Buis, J., Setzer, A., Vermote, E., Reagan, J., Kaufman, Y., and Nakajima, T.: AERONET – A federated instrument network and data archive for aerosol characterization, *Remote Sens. Environ.*, 66, 1–16, 1998.
- Hsu, N. C., Jeong, M. J., Bettenhausen, C., Sayer, A. M., Hansell, R., Seftor, C. S., Huang, J., and Tsay, S. C.: Enhanced Deep Blue aerosol retrieval algorithm: The second generation, *J. Geophys. Res.-Atmos.*, 118, 9296–9315, doi:10.1002/jgrd.50712, 2013.
- Ichoku, C., Levy, R., Kaufman, Y. J., Remer, L. A., Li, R. R., Martins, V. J., Holben, B. N., Abuhassan, N., Slutsker, I., and Eck, T. F.: Analysis of the performance characteristics of the five-channel Microtops II Sun photometer for measuring aerosol optical thickness and precipitable water vapor, *J. Geophys. Res.-Atmos.*, 107, AAC5-1–AAC5-17, 2002.
- Jackson, J. M., Liu, H., Laszlo, I., Kondragunta, S., Remer, L. A., Huang, J., and Huang, H. C.: Suomi-NPP VIIRS aerosol algorithms and data products, *J. Geophys. Res.-Atmos.*, 118, 12673–12689, 2013.
- Lee, J., Kim, J., Song, C. H., Ryu, J.-H., Ahn, Y.-H., and Song, C.: Algorithm for retrieval of aerosol optical properties over the ocean from the Geostationary Ocean Color Imager, *Remote Sens. Environ.*, 114, 1077–1088, 2010.
- Levy, R. C., Remer, L. A., and Dubovik, O.: Global aerosol optical properties and application to Moderate Resolution Imaging Spectroradiometer aerosol retrieval over land, *J. Geophys. Res.-Atmos.*, 112, D13210, doi:10.1029/2006jd007815, 2007.
- Levy, R. C., Remer, L. A., Kleidman, R. G., Mattoo, S., Ichoku, C., Kahn, R., and Eck, T. F.: Global evaluation of the Collection 5 MODIS dark-target aerosol products over land, *Atmos. Chem. Phys.*, 10, 10399–10420, doi:10.5194/acp-10-10399-2010, 2010.
- Levy, R. C., Mattoo, S., Munchak, L. A., Remer, L. A., Sayer, A. M., Patadia, F., and Hsu, N. C.: The Collection 6 MODIS aerosol products over land and ocean, *Atmos. Meas. Tech.*, 6, 2989–3034, doi:10.5194/amt-6-2989-2013, 2013.
- Li, C., Lau, A.-H., Mao, J., and Chu, D. A.: Retrieval, validation, and application of the 1-km aerosol optical depth from MODIS measurements over Hong Kong, *IEEE Geosci. Remote S.*, 43, 2650–2658, 2005.
- Lim, S. S., Vos, T., Flaxman, A. D., Danaei, G., Shibuya, K., Adair-Rohani, H., AlMazroa, M. A., Amann, M., Anderson, H. R., and Andrews, K. G.: A comparative risk assessment of burden of disease and injury attributable to 67 risk factors and risk factor clusters in 21 regions, 1990–2010: a systematic analysis for the Global Burden of Disease Study 2010, *The Lancet*, 380, 2224–2260, 2013.
- Liu, H., Remer, L. A., Huang, J., Huang, H. C., Kondragunta, S., Laszlo, I., Oo, M., and Jackson, J. M.: Preliminary evaluation of S-NPP VIIRS aerosol optical thickness, *J. Geophys. Res.-Atmos.*, 119, 3942–3962, 2014.
- Liu, Y., Franklin, M., Kahn, R., and Koutrakis, P.: Using aerosol optical thickness to predict ground-level PM 2.5 concentrations in the St. Louis area: a comparison between MISR and MODIS, *Remote Sens. Environ.*, 107, 33–44, 2007.
- Ma, Z., Hu, X., Huang, L., Bi, J., and Liu, Y.: Estimating ground-level PM2.5 in China using satellite remote sensing, *Environ. Sci. Technol.*, 48, 7436–7444, 2014.
- Morys, M., Mims, F. M., Hagerup, S., Anderson, S. E., Baker, A., Kia, J., and Walkup, T.: Design, calibration, and performance of MICROTOS II handheld ozone monitor and Sun photometer, *J. Geophys. Res.-Atmos.*, 106, 14573–14582, 2001.
- Munchak, L. A., Levy, R. C., Mattoo, S., Remer, L. A., Holben, B. N., Schafer, J. S., Hostetler, C. A., and Ferrare, R. A.: MODIS 3 km aerosol product: applications over land in an urban/suburban region, *Atmos. Meas. Tech.*, 6, 1747–1759, doi:10.5194/amt-6-1747-2013, 2013.
- Ohara, T., Akimoto, H., Kurokawa, J., Horii, N., Yamaji, K., Yan, X., and Hayasaka, T.: An Asian emission inventory of anthropogenic emission sources for the period 1980–2020, *Atmos. Chem. Phys.*, 7, 4419–4444, doi:10.5194/acp-7-4419-2007, 2007.
- Otter, L., Scholes, R., Dowty, P., Privette, J., Caylor, K., Ringrose, S., Mukelabai, M., Frost, P., Hanan, N., and Totolo, O.: The Southern African regional science initiative (SAFARI 2000): wet season campaigns, *S. Afr. J. Sci.*, 98, 131–137, 2002.
- Park, M. E., Song, C. H., Park, R. S., Lee, J., Kim, J., Lee, S., Woo, J.-H., Carmichael, G. R., Eck, T. F., Holben, B. N., Lee, S.-S., Song, C. K., and Hong, Y. D.: New approach to monitor transboundary particulate pollution over Northeast Asia, *Atmos. Chem. Phys.*, 14, 659–674, doi:10.5194/acp-14-659-2014, 2014.
- Remer, L. A., Mattoo, S., Levy, R. C., and Munchak, L. A.: MODIS 3 km aerosol product: algorithm and global perspective, *Atmos. Meas. Tech.*, 6, 1829–1844, doi:10.5194/amt-6-1829-2013, 2013.
- Sano, I., Mukai, S., Holben, B. N., Nakata, M., Yonemitsu, M., Sugimoto, N., Fujito, T., Hiraki, T., Iguchi, N., Kozai, K., Kuji, M., Muramatsu, K., Okada, Y., Sadanaga, Y., Tohno, S., Toyazaki, Y., and Yamamoto, K.: DRAGON-West Japan campaign in 2012:

- regional aerosol measurements over Osaka, *Proc. SPIE*, 8523, 8523–8555, 2012.
- Seo, S., Kim, J., Lee, H., Jeong, U., Kim, W., Holben, B. N., Kim, S.-W., Song, C. H., and Lim, J. H.: Estimation of PM<sub>10</sub> concentrations over Seoul using multiple empirical models with AERONET and MODIS data collected during the DRAGON-Asia campaign, *Atmos. Chem. Phys.*, 15, 319–334, doi:10.5194/acp-15-319-2015, 2015.
- Strickland, M., Hao, H., Hu, X., Chang, H., Darrow, L., and Liu, Y.: Pediatric Emergency Visits and Short-Term Changes in PM<sub>2.5</sub> Concentrations in the US State of Georgia, *Environ. Health Persp.*, doi:10.1289/ehp.1509856, 2015.
- Tiwari, S. and Singh, A.: Variability of aerosol parameters derived from ground and satellite measurements over Varanasi located in the Indo-Gangetic Basin, *Aerosol. Air Qual. Res.*, 13, 627–638, 2013.
- Vermote, E., Justice, C., and Csiszar, I.: Early evaluation of the VIIRS calibration, cloud mask and surface reflectance Earth data records, *Remote Sens. Environ.*, 148, 134–145, 2014.
- Xu, J.-W., Martin, R. V., van Donkelaar, A., Kim, J., Choi, M., Zhang, Q., Geng, G., Liu, Y., Ma, Z., Huang, L., Wang, Y., Chen, H., Che, H., Lin, P., and Lin, N.: Estimating ground-level PM<sub>2.5</sub> in eastern China using aerosol optical depth determined from the GOCI satellite instrument, *Atmos. Chem. Phys.*, 15, 13133–13144, doi:10.5194/acp-15-13133-2015, 2015.